Available online at www.sciencedirect.com
SCIENCE DIRECT®
ELSEVIER
Nuclear Instruments and Methods in Physics Research B 234 (2005) 321–332
NIM B
Beam Interactions with Materials & Atoms
www.elsevier.com/locate/nimb

A study of cosmic ray secondaries induced by the *Mir* space station using AMS-01

M. Aguilar [a], J. Alcaraz [a], J. Allaby [b], B. Alpat [c], G. Ambrosi [d,c], H. Anderhub [e], L. Ao [f], A. Arefiev [g], P. Azzarello [d], E. Babucci [c], L. Baldini [h,i], M. Basile [h], D. Barancourt [j], F. Barao [k,l], G. Barbier [j], G. Barreira [k], R. Battiston [c], R. Becker [i], U. Becker [i], L. Bellagamba [h], P. Béné [d], J. Berdugo [a], P. Berges [i], B. Bertucci [c], A. Biland [e], S. Bizzaglia [c], S. Blasko [c], G. Boella [m], M. Boschini [m], M. Bourquin [d], L. Brocco [h], G. Bruni [h], M. Buénerd [j], J.D. Burger [i], W.J. Burger [c], X.D. Cai [i], C. Camps [n], P. Cannarsa [e], M. Capell [i], G. Carosi [i], D. Casadei [h], J. Casaus [a], G. Castellini [o,h], C. Cecchi [c], Y.H. Chang [p], H.F. Chen [q], H.S. Chen [r], Z.G. Chen [f], N.A. Chernoplekov [s], T.H. Chiueh [p], K. Cho [t], M.J. Choi [u], Y.Y. Choi [u], Y.L. Chuang [v], F. Cindolo [h], V. Commichau [n], A. Contin [h], E. Cortina-Gil [d], M. Cristinziani [d], J.P. da Cunha [w], T.S. Dai [i], C. Delgado [a], B. Demirköz [i], J.D. Deus [l], N. Dinu [c,1], L. Djambazov [e], I. D'Antone [h], Z.R. Dong [x], P. Emonet [d], J. Engelberg [y], F.J. Eppling [i], T. Eronen [z], G. Esposito [c], P. Extermann [d], J. Favier [aa], E. Fiandrini [c], P.H. Fisher [i], G. Fluegge [n], N. Fouque [aa], Yu. Galaktionov [g,i], M. Gervasi [m], P. Giusti [h], D. Grandi [m], O. Grimm [e], W.Q. Gu [x], K. Hangarter [n], A. Hasan [e], R. Henning [i,*,2], V. Hermel [aa], H. Hofer [e], M.A. Huang [v], W. Hungerford [e], M. Ionica [c,1], R. Ionica [c,1], M. Jongmanns [e], K. Karlamaa [y], W. Karpinski [ab], G. Kenney [e], J. Kenny [c], D.H. Kim [t], G.N. Kim [t], K.S. Kim [u], M.Y. Kim [u], A. Klimentov [i,g], R. Kossakowski [aa], V. Koutsenko [i,g], M. Kraeber [e], G. Laborie [j], T. Laitinen [z], G. Lamanna [c], E. Lanciotti [a],

[*] Corresponding author. Tel.: +1 5104867121; fax: +1 5104866738.
E-mail address: rhenning@lbl.gov (R. Henning).
[1] Permanent address: HEPPG, Univ. of Bucharest, Romania.
[2] Now at Lawrence Berkeley National Laboratory, Berkeley, CA 94720, USA.

0168-583X/$ - see front matter
doi:10.1016/j.nimb.2005.01.015

G. Laurenti [h], A. Lebedev [i], C. Lechanoine-Leluc [d], M.W. Lee [t], S.C. Lee [v], G. Levi [h], P. Levtchenko [c,3], C.L. Liu [ac], H.T. Liu [r], I. Lopes [w], G. Lu [f], Y.S. Lu [r], K. Lübelsmeyer [ab], D. Luckey [i], W. Lustermann [e], C. Maña [a], A. Margotti [h], F. Mayet [j], R.R. McNeil [ad], B. Meillon [j], M. Menichelli [c], A. Mihul [ae], B. Monreal [i], A. Mourao [l], A. Mujunen [y], F. Palmonari [h], A. Papi [c], H.B. Park [t], W.H. Park [t], M. Pauluzzi [c], F. Pauss [e], E. Perrin [d], A. Pesci [h], A. Pevsner [af], M. Pimenta [k,l], V. Plyaskin [g], V. Pojidaev [g], M. Pohl [d], V. Postolache [c,1], N. Produit [d], P.G. Rancoita [m], D. Rapin [d], F. Raupach [ab], D. Ren [e], Z. Ren [v], M. Ribordy [d], J.P. Richeux [d], E. Riihonen [z], J. Ritakari [y], S. Ro [t], U. Roeser [e], C. Rossin [j], R. Sagdeev [ag], D. Santos [j], G. Sartorelli [h], C. Sbarra [h], S. Schael [ab], A. Schultz von Dratzig [ab], G. Schwering [ab], G. Scolieri [c], E.S. Seo [ag], J.W. Shin [t], E. Shoumilov [g], V. Shoutko [i], R. Siedling [ab], D. Son [t], T. Song [x], M. Steuer [i], G.S. Sun [x], H. Suter [e], X.W. Tang [r], Samuel C.C. Ting [i], S.M. Ting [i], M. Tornikoski [y], J. Torsti [z], J. Trümper [ah], J. Ulbricht [e], S. Urpo [y], E. Valtonen [z], J. Vandenhirtz [ab], F. Velcea [c,1], E. Velikhov [s], B. Verlaat [e,4], I. Vetlitsky [g], F. Vezzu [j], J.P. Vialle [aa], G. Viertel [e], D. Vité [d], H. Von Gunten [e], S. Waldmeier Wicki [e], W. Wallraff [ab], B.C. Wang [ac], J.Z. Wang [f], Y.H. Wang [v], K. Wiik [y], C. Williams [h], S.X. Wu [i,p], P.C. Xia [x], J.L. Yan [f], L.G. Yan [x], C.G. Yang [r], J. Yang [u], M. Yang [r], S.W. Ye [q,5], P. Yeh [v], Z.Z. Xu [q], H.Y. Zhang [ai], Z.P. Zhang [q], D.X. Zhao [x], G.Y. Zhu [r], W.Z. Zhu [f], H.L. Zhuang [r], A. Zichichi [h], B. Zimmermann [e], P. Zuccon [c]

[a] *Centro de Investigaciones Energéticas, Medioambientales y Tecnológicas, CIEMAT, E-28040 Madrid, Spain*[6]
[b] *European Laboratory for Particle Physics, CERN, CH-1211 Geneva 23, Switzerland*
[c] *INFN-Sezione di Perugia and Universitá Degli Studi di Perugia, I-06100 Perugia, Italy*[7]
[d] *University of Geneva, CH-1211 Geneva 4, Switzerland*
[e] *Eidgenössische Technische Hochschule, ETH Zürich, CH-8093 Zürich, Switzerland*
[f] *Chinese Academy of Launching Vehicle Technology, CALT, 100076 Beijing, China*
[g] *Institute of Theoretical and Experimental Physics, ITEP, Moscow 117259, Russia*
[h] *University of Bologna and INFN-Sezione di Bologna, I-40126 Bologna, Italy*[7]
[i] *Massachusetts Institute of Technology, Cambridge, MA 02139, USA*
[j] *Institut des Sciences Nucleaires, IN2P3/CNRS, F-38026 Grenoble, France*
[k] *Laboratorio de Instrumentacao e Fisica Experimental de Particulas, LIP, P-1000 Lisboa, Portugal*
[l] *Instituto Superior Técnico, IST, P-1096 Lisboa, Portugal*
[m] *INFN-Sezione di Milano, I-20133 Milan, Italy*[7]
[n] *III. Physikalisches Institut, RWTH, D-52056 Aachen, Germany*[8]
[o] *CNR–IROE, I-50125 Florence, Italy*
[p] *National Central University, Chung-Li 32054, Taiwan*

[3] Permanent address: Nuclear Physics Institute, St. Petersburg, Russia.
[4] Now at National Institute for High Energy Physics, NIKHEF, NL-1009 DB Amsterdam, The Netherlands.
[5] Supported by ETH Zürich.
[6] Also supported by the Comisión Interministerial de Ciencia y Tecnología.
[7] Also supported by the Italian Space Agency.
[8] Supported by the Deutsches Zentrum für Luft– und Raumfahrt, DLR.

[q] Chinese University of Science and Technology, USTC, Hefei, Anhui 230 029, China[9]
[r] Institute of High Energy Physics, IHEP, Chinese Academy of Sciences, 100039 Beijing, China[9]
[s] Kurchatov Institute, Moscow 123182, Russia
[t] CHEP, Kyungpook National University, 702-701 Daegu, Republic of Korea
[u] Ewha Womens University, 120-750 Seoul, Republic of Korea
[v] Academia Sinica, Taipei 11529, Taiwan
[w] Laboratorio de Instrumentacao e Fisica Experimental de Particulas, LIP, P-3000 Coimbra, Portugal
[x] Institute of Electrical Engineering, IEE, Chinese Academy of Sciences, 100080 Beijing, China
[y] Helsinki University of Technology, FIN-02540 Kylmala, Finland
[z] University of Turku, FIN-20014 Turku, Finland
[aa] Laboratoire d'Annecy-le-Vieux de Physique des Particules, LAPP, F-74941 Annecy-le-Vieux CEDEX, France
[ab] I. Physikalisches Institut, RWTH, D-52056 Aachen, Germany[8]
[ac] Chung–Shan Institute of Science and Technology, Lung-Tan, Tao Yuan 325, Taiwan
[ad] Louisiana State University, Baton Rouge, LA 70803, USA
[ae] Institute of Microtechnology, Politechnica University of Bucharest and University of Bucharest, R-76900 Bucharest, Romania
[af] Johns Hopkins University, Baltimore, MD 21218, USA
[ag] University of Maryland, College Park, MD 20742, USA
[ah] Max–Planck Institut für extraterrestrische Physik, D-85740 Garching, Germany
[ai] Center of Space Science and Application, Chinese Academy of Sciences, 100080 Beijing, China

Received 24 June 2004; received in revised form 23 December 2004
Available online 17 March 2005

Abstract

The Alpha Magnetic Spectrometer (AMS-02) is a high energy particle physics experiment that will study cosmic rays in the ~100 MeV to 1 TeV range and will be installed on the International Space Station (ISS) for at least 3 years. A first version of AMS-02, AMS-01, flew aboard the space shuttle *Discovery* from June 2 to June 12, 1998, and collected 10^8 cosmic ray triggers. Part of the *Mir* space station was within the AMS-01 field of view during the four day *Mir* docking phase of this flight. We have reconstructed an image of this part of the *Mir* space station using secondary π^- and μ^- emissions from primary cosmic rays interacting with *Mir*. This is the first time this reconstruction was performed in AMS-01, and it is important for understanding potential backgrounds during the 3 year AMS-02 mission.

PACS: 13.85.Tp; 25.40.Sc; 29.30.Aj; 95.55.Vj; 95.85.Ry

Keywords: Cosmic rays; Spallation; AMS; Mir; Space shuttle

1. Introduction

The Alpha Magnetic Spectrometer (AMS-02) is a high energy particle physics experiment to be installed on the International Space Station (ISS). It will be mounted on an external truss of the ISS for at least three years and collect ~10^{11} cosmic ray events in the ~100 MeV to 1 TeV range. The launch is currently scheduled for 2007. A first version of the AMS-02 experiment, AMS-01, flew aboard the space shuttle *Discovery* from June 2 to June 12, 1998 (Fig. 1). Analysis of the 97 million cosmic ray triggers collected by AMS-01 during the flight provided valuable measurements of cosmic rays in near earth orbit [1–5]. *Discovery* was docked with the space station *Mir* for 95 of the 235 h of the AMS-01 flight (Fig. 2). This paper presents a reconstructed image of the part of the

[9] Supported by the National Natural Science Foundation of China.

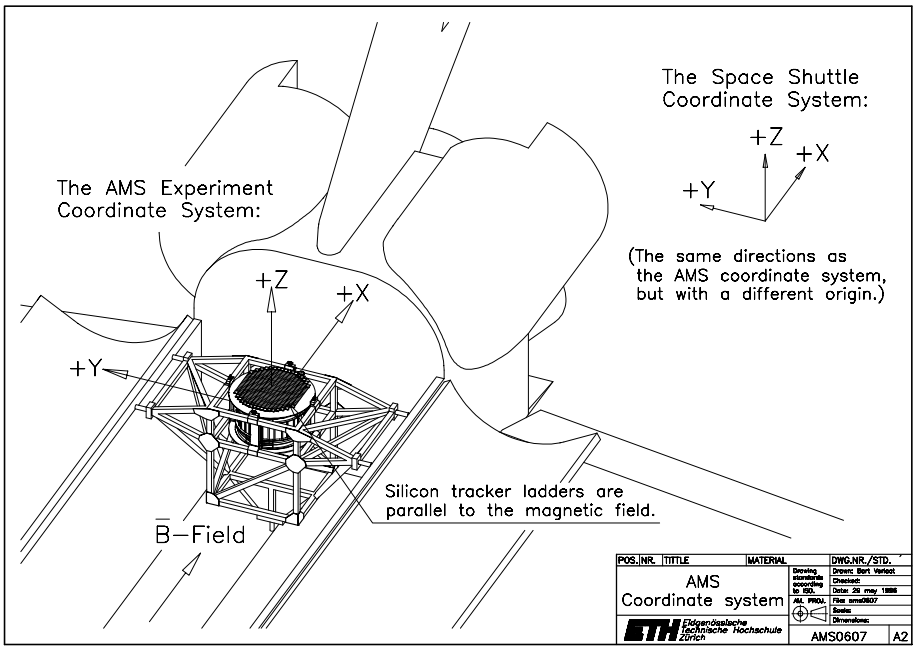

Fig. 1. Diagram of AMS-01 in the payload bay of *Discovery*. The space shuttle and AMS-01 coordinate systems are shown.

Mir space station that was within the AMS-01 field of view during the flight. The image is generated from secondary π^- and μ^- emissions detected by AMS-01 that were produced by primary cosmic rays interacting with *Mir*.

2. The AMS-01 experiment

A schematic of the AMS-01 detector is shown in Fig. 3. AMS-01's core components were a time-of-flight hodoscope (TOF) that determined the cosmic ray's velocity ($\beta = v/c$), and a silicon microstrip tracking system inside a permanent magnet that measured particle rigidity (R) and charge sign. The TOF resolution was $\delta\beta/\beta \approx 3\%$ and the tracker rigidity range was 100 MV to 200 GV for protons with an optimal resolution of $\delta R/R \approx 7\%$ at 10 GeV/c. Tracker resolution was limited by multiple scattering and the bending power of the magnet at low and high rigidities, respectively. Energy deposits in the TOF paddles and tracker silicon sensors determined the particle's charge, and the probability for charge misidentification between $Z = 1$ and $Z = 2$ particles was estimated to be $<10^{-4}$. An anti-coincidence counter (ACC) inside the barrel of the magnet vetoed events with secondary particles that missed the TOF detector. An Aerogel Threshold Čerenkov detector provided additional particle identifying capability. The trigger for recording an event consisted of a coincidence between the upper and lower TOF planes and an anticoincidence with the ACC scintillators. Aguilar et al. [7] has a detailed description of the AMS-01 hardware and triggering scheme.

Ionization charge from energy deposits of cosmic rays traversing the TOF scintillators and silicon track sensors were digitized and recorded as hits by the readout electronics. An offline analysis program reconstructed events from these hits after the flight. It performed a three dimensional linear χ^2 fit to the time measurements from the TOF and the reconstructed pathlength of the cosmic ray trajectory in the detector. The inverse slope of the fit yielded the cosmic ray's velocity (β). The cosmic ray's trajectory inside the tracking volume (magnet) was reconstructed from the hits in

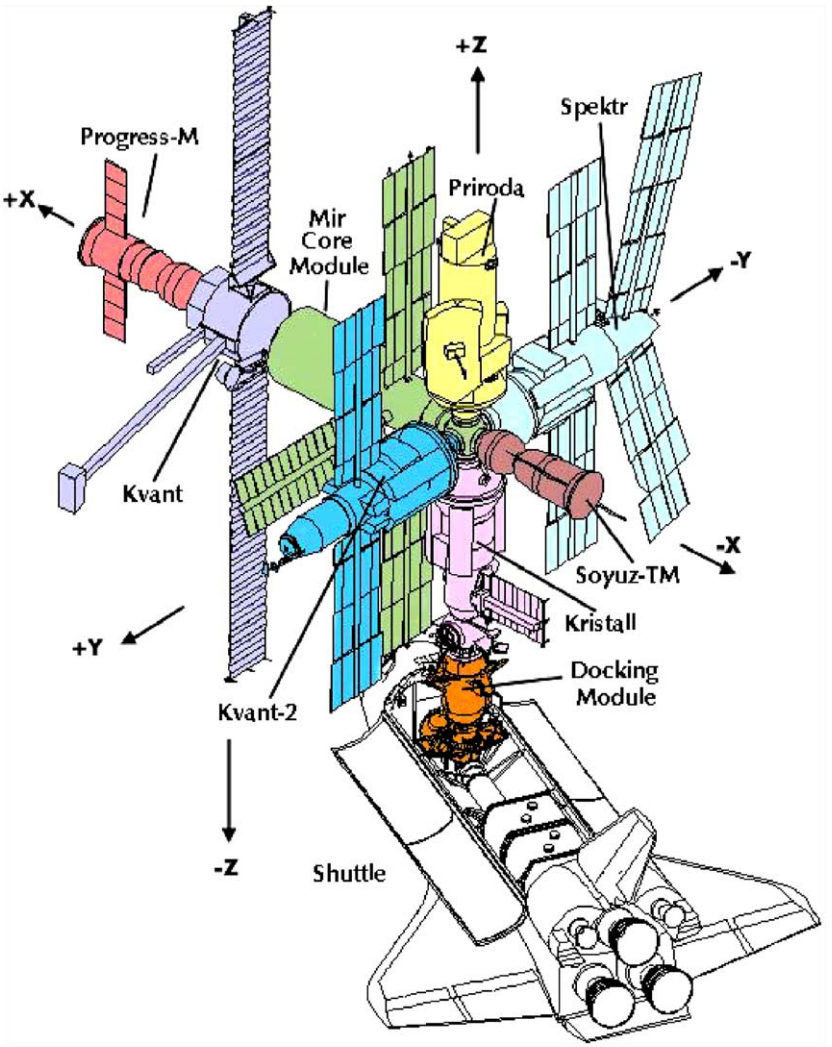

Fig. 2. The space station *Mir* and space shuttle shown in a docked position. The distance from the top of the *Priroda* module to the shuttle payload bay is 30 m. The figure is to scale. Note that there is a non-zero angle between the shuttle x-axis (Fig. 1) and the *Mir* x-axis. Figure courtesy of NASA and taken from [6].

the tracker by a sophisticated tracking algorithm described in [8]. It included the effects of multiple scattering and the inhomogeneous magnetic field. The tracking algorithm yielded five quantities, $(x, y, \theta, \phi, 1/R)$, where (x, y) is the impact point on the first tracker plane the particle encounters, θ and ϕ describes the incident direction of the particle relative to the AMS-01 coordinate system, and R is the rigidity. The particle mass was determined from R and β via

$$m = \frac{|Z|R}{c}\sqrt{\beta^{-2} - 1}, \tag{1}$$

where $p = R$ for $Z = 1$ particles.

3. *Mir* as "Seen" by AMS-01

The precision silicon tracker determined the incident direction of cosmic rays to better than a degree. The incident directions of cosmic rays were

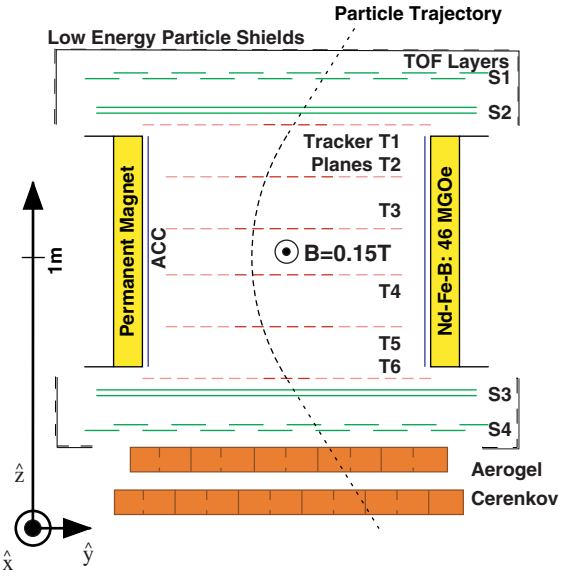

Fig. 3. A schematic cross-section of the AMS-01 detector showing the subdetectors.

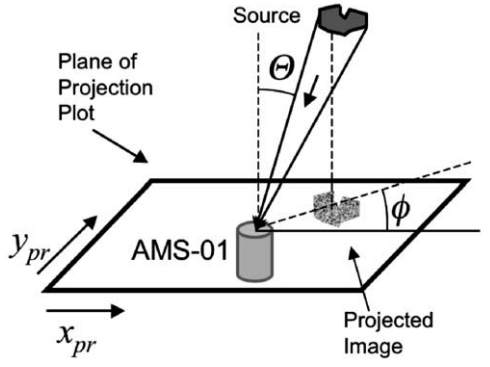

Fig. 4. A schematic illustrating how the arrival directions of incoming cosmic rays are projected onto a plane such that images of co-moving cosmic ray sources can be created.

binned according to a projection on an x–y plane, such that an "image" is generated (Fig. 4). Regions of the sky overhead to AMS-01 were projected one-to-one to an x–y plane using the standard transformation of arrival direction:

$$x_{\rm pr} = -\sin\theta\cos\phi,$$
$$y_{\rm pr} = \sin\theta\sin\phi,$$

where θ is the polar angle, and ϕ is the azimuthal angle of the incoming cosmic ray.

Fig. 5 compares projection plots of $x_{\rm pr}$ versus $y_{\rm pr}$ for downward-going $Z = -1$ events when *Discovery* was docked and not docked with *Mir*. During the docking phase the precession of *Mir* and *Discovery* caused AMS-01 to cover most of the sky. Hence, in the absence of a co-moving source, we would expect a uniform distribution of incident directions for cosmic rays, convoluted with the decreasing acceptance of AMS-01 at larger polar angle. However, we observe a significant excess of events from a specific region on the left of the *Mir* docking phase projection plot. This region covered 0.7% of the AMS-01 acceptance.

As we will show, this excess is due to the *Mir* space station. The vertical stripes are events that did not have reconstructible tracks in the non-bending plane of the tracker. The track in the non-bending plane was recovered using the spatial data from the TOF hodoscope. Hence, the vertical stripes are artifacts of the reconstruction and not physical.

Fig. 6 shows projection plots for upward-going particles. No excess is observed in this upward-going sample, although faint structures do appear, possibly due to bulkheads and support members in the space shuttle airframe and the lower part of the Unique Support Structure of AMS-01.

Cuts were applied to improve the mass determination of impinging cosmic rays. They required agreement between the particle trajectories computed from the TOF and tracker, imposed upper limits on the χ^2 of the track and velocity fits, and rejected events with bad tracker strips, TOF paddles, and spurious hits. These cuts rejected events that suffered hard scattering or interactions in the detector material. The resulting mass spectra for $Z = -1$ events are shown in Fig. 7. Events that have measured $\beta > 1$ due to the finite resolution of the TOF had a "mass" computed, as per Eq. (1), with a transformed value of velocity: $1/\beta' = 2 - 1/\beta$. These events were tagged by assigning their computed mass a negative sign. Electrons have $\beta = 1$ within the TOF resolution at the energies of interest here, hence we expect the measured mass for e^- to be distributed symmetrically around $m = 0$ GeV/c^2. This distribution is indeed observed

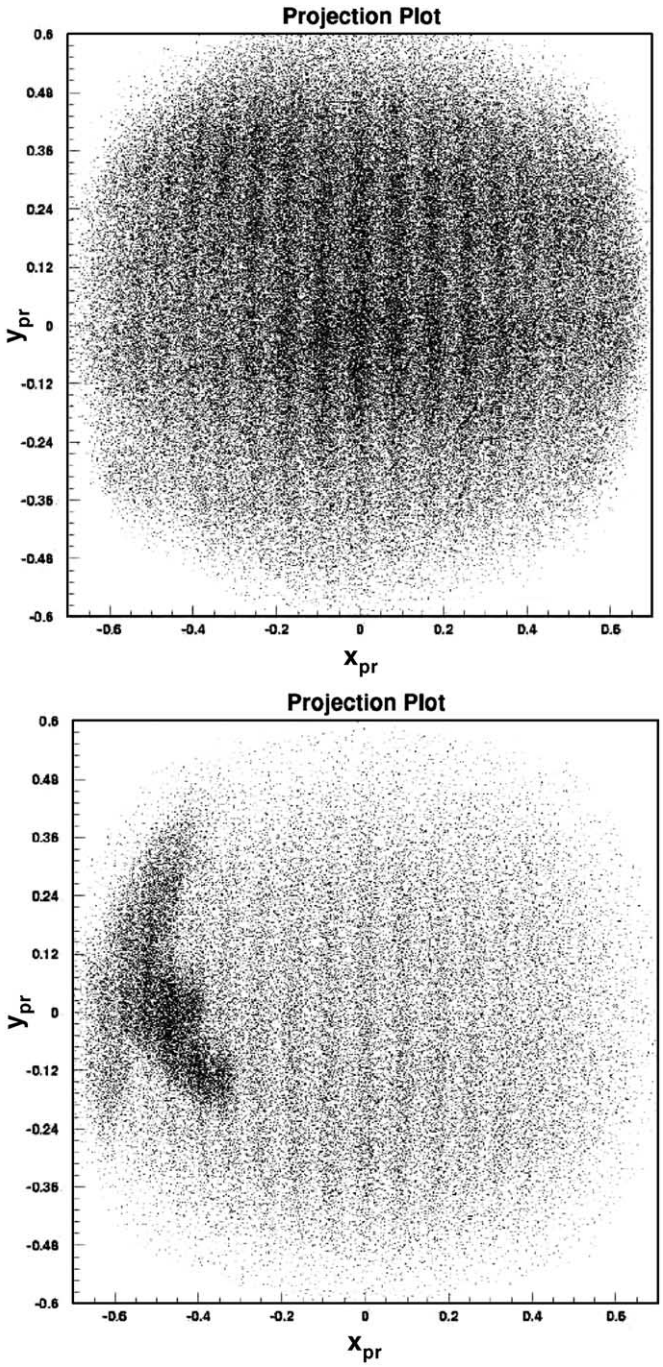

Fig. 5. Projection plots for downward-going particles with measured charge $Z = -1$ when *Discovery* was not docked (top) and docked (bottom) with *Mir*. Note the relative excess of events from a clearly defined region during the *Mir* docking phase on the left side of the projection plot. The number of events in the top and bottom plots are 674 000 and 647 000, respectively. The corresponding rates are 1.42 s^{-1} (top) and 1.87 s^{-1} (bottom). The rate of events from the excess flux region on the bottom plot is 0.064 s^{-1} during the docking phase and 0.010 s^{-1} outside the docking phase. The excess flux region contains 22000 $Z = -1$ events. The vertical stripes are explained in the text.

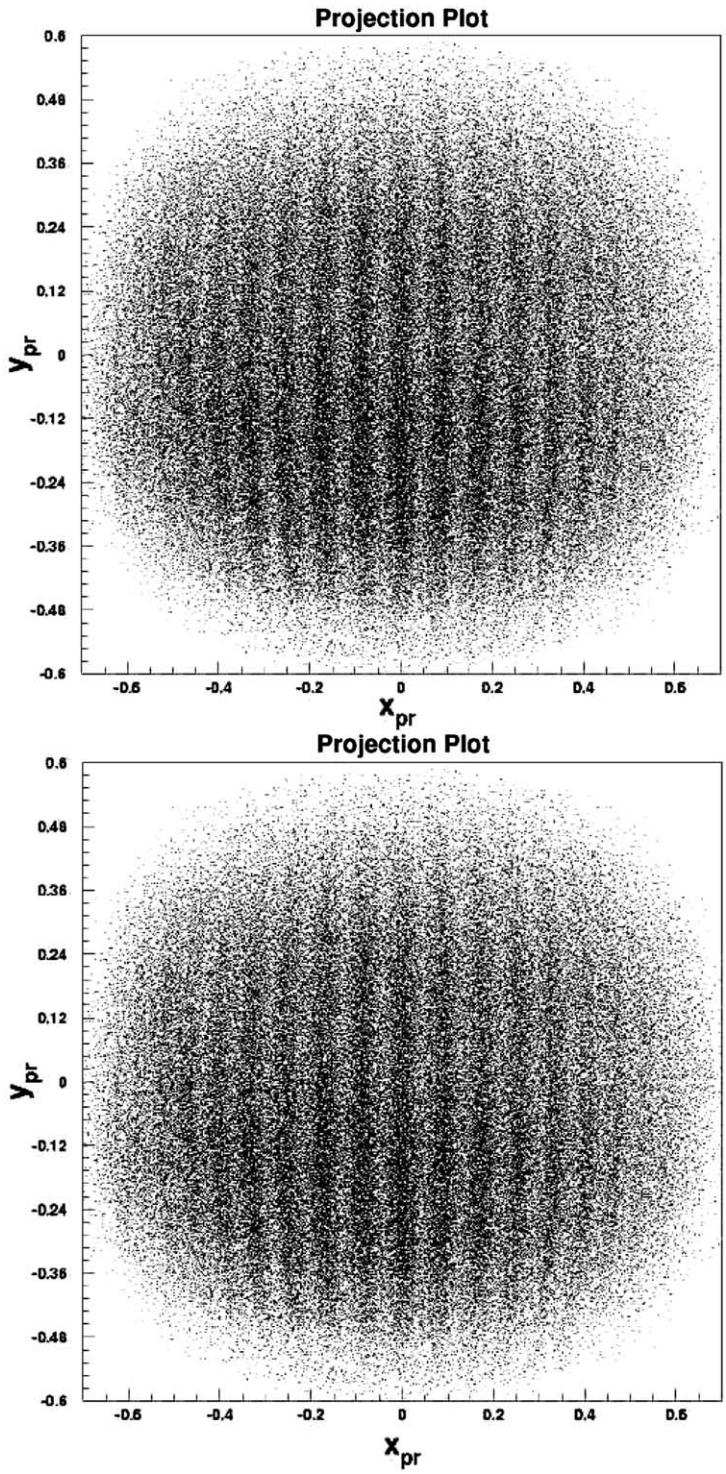

Fig. 6. Projection plots for upward-going particles with measured $Z = -1$ when *Discovery* was not docked (top) and docked (bottom) with *Mir*. No excess event regions are present during the *Mir* docking phase. The plot on the top has 538 000 events and the one on the bottom has 389 000. The corresponding event rate is 1.1 event s^{-1}.

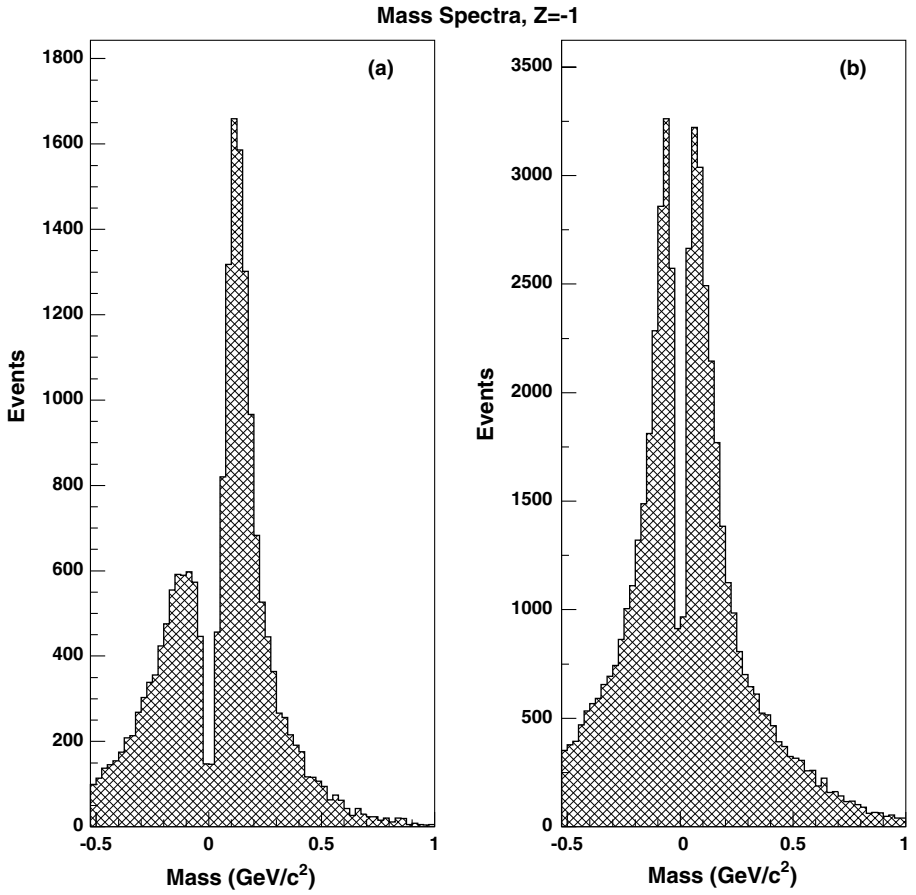

Fig. 7. Mass spectra for downward-going $Z = -1$ events from the excess flux region (a) and not from the excess flux region (b) in Fig. 5. Note the large excess of events with masses consistent with μ^- and π^- from the excess region. The meaning of negative masses are explained in the text.

in the mass spectra from cosmic rays not originating from the excess on the projection plot (Fig. 7(b)). This is not surprising, since $Z = -1$ cosmic rays are dominated by e^-. However, there is a large excess of events in the $0.1 - 0.2$ GeV/c^2 range from the flux excess region. A probable source of this excess is π^- and μ^- produced by high energy cosmic ray nuclei, primarily protons and Helium, interacting hadronically with atomic nuclei in an object in the vicinity of the shuttle. The cosmic ray proton flux is $\sim$100 times that of the $Z = -1$ electron flux, hence spallation products from cosmic ray protons could contribute significantly to the $Z = -1$ flux.

The mass-resolved μ^- and π^- events shown in the mass histograms have momentum in the $0.2 - 0.4$ GeV/c range. This indicates that the comoving source of the excess cannot be further than several hundred meters, since for μ^- and π^- we have $c\tau = 660$ m and $c\tau = 7.8$ m, respectively.

4. Discussion

A one-to-one correspondence between the excess seen in Fig. 5 and the physical layout of the *Mir* space station was found. Fig. 8 shows a picture of *Mir* taken from a porthole of a

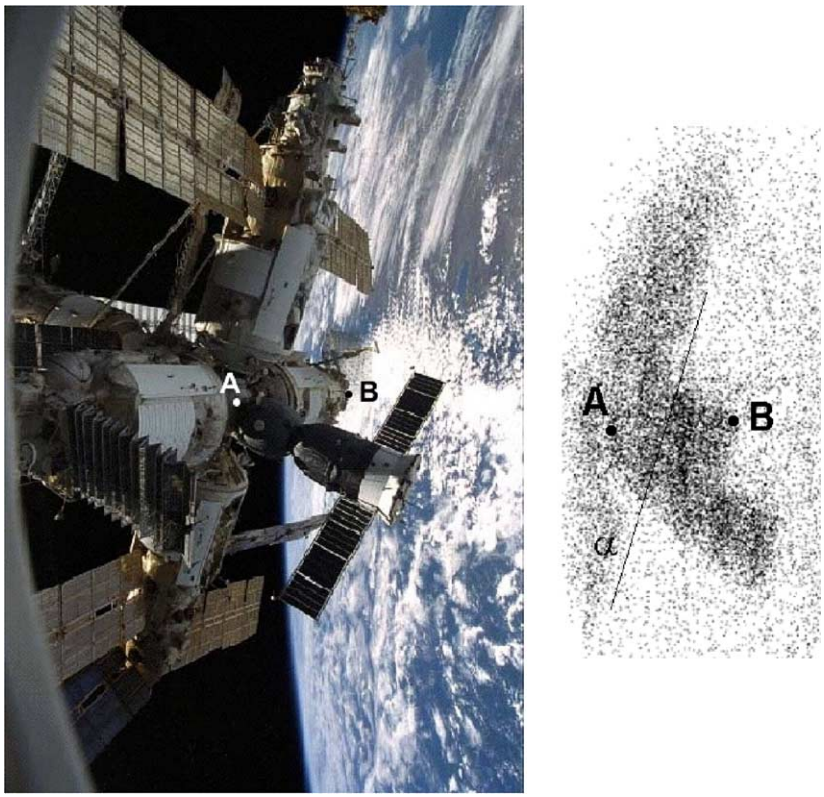

Fig. 8. The picture on the left shows the space station *Mir* as seen from a porthole in a SpaceHab module in the back of the payload bay of *Endeavour* during STS-89. Visible are the *Spektr* (pointing upwards), *Priroda* (pointing to earth), *Soyuz* (black and white, pointing to right), *Kvant-2* (pointing down) and *Kristall* (pointing to left) modules. The picture was taken from a location similar to that of AMS-01 relative to *Mir*. The image on the right is a zoom of the projection plot for $Z = -1$ events. Note the striking correspondence if the solar panels on the picture are ignored. The points *A* and *B* and the angle α are discussed in the text. Image on left is courtesy of NASA and taken from [6].

SpaceHab module at the rear of the payload bay of the shuttle *Endeavour* when it docked with *Mir* during an earlier mission (STS-89). The SpaceHab porthole during this flight was in a similar location as AMS-01 during the *Discovery* flight docking phase; hence the view in the picture is similar to the view of *Mir* from AMS-01. Also shown is a zoom of the excess events region in the projection plot. The correspondence between the two images is striking if the solar panels in the picture are ignored. We clearly see the *Soyuz* spacecraft projecting to the lower right, as well as the *Priroda*, *Spektr* and *Kvant-2* modules. The solar panels presented much less material for spallation, and μ^-/π^- emission from them are not visible in the projection plot, as will be shown later.

As a check whether we are indeed seeing *Mir*, two points were chosen by inspection on the projection plot that appear to correspond to the node of the *Mir* station, labeled point *A*, and the top (furthest away) part of the *Priroda* module, labeled point *B*. The polar angles of the points relative to the AMS-01 *z*-axis, as well as the angle between the shuttle's *x*-axis and *Mir*'s *x*-axis, α, were estimated from the projection plots. These quantities were also computed independently using the dimensions of the *Mir* modules and the space shuttle, taken from [6]. The estimates of *A*, *B* and α from the projection plots are compared with the

Table 1
Comparison of measurements from projection plots to engineering specifications from [6]

Quantity	Projection plot	Specifications and images
Polar angle of A	$54.5 \pm 2.0°$	$51.5 \pm 1.5°$
Polar angle of B	$67.6 \pm 1.6°$	$66.0 \pm 1.5°$
α	$25.7 \pm 1.6°$	$26.0 \pm 1.6°$

The errors in the second column are the estimated uncertainty in locating points A and B by eye. The errors in the third column are the uncertainties due to the location of AMS-01 relative to *Mir*.

computed values in Table 1. They are in excellent agreement, leading us to conclude that the excess seen in the projection plot is indeed part of the *Mir* space station.

The detected μ^- and π^- flux is a complex convolution of several energy and direction-dependent functions: the time-averaged incident cosmic ray flux, the material distribution and composition of the *Mir* space station, the π^- production cross-section, the survival probability of the π^- and μ^-, the detector acceptance and finally the reconstruction software efficiency. The evaluation of this complex expression is beyond the scope of this paper; however, a simple estimate of the incident cosmic ray energy can be made from the data as a consistency check.

The average reconstructed "ambient" event rate from the region covered by *Mir* when the shuttle is not docked with it is measured to be $0.27\,s^{-1}$ and $0.010\,s^{-1}$ for $Z = +1$ and $Z = -1$ events, respectively. The rate for $Z = -1$ events in the same region increases to $0.064\,s^{-1}$ during the docking phase, hence the events from *Mir* dominate in this region during the docking phase and occur at a rate of $\approx 0.06\,s^{-1}$. This is $\approx 20\%$ of the ambient $Z = +1$ rate. If we approximate *Mir* as a target of 10 cm thick aluminum [10] and the inelastic cross-section for protons on aluminum as $45A^{0.7}$ mbarn, where $A = 26$ for aluminum [9], then it can be shown that $\approx 25\%$ of cosmic ray protons will interact inelastically with *Mir*. Although ^{4}He nuclei compose only 20% of the cosmic ray flux at these energies, $\approx 50\%$ will interact with *Mir*, at a rate $50\% \times 25\% = 13\%$ that of the proton flux. Hence, the rate of cosmic ray ^{4}He and proton interactions in the region covered by *Mir* is $25 + 13 \approx 40\%$ that of the ambient proton flux from the same region. This implies an observed, average π^- multiplicity of $20/40 = 0.5$ per interaction, assuming the detection efficiency for $Z = -1$ and $Z = +1$ particles are the same, and that all produced π^- reach AMS-01 as $Z = -1$ particles. This multiplicity requires an incident momentum for the cosmic ray protons and ^{4}He of ≈ 5 GeV/c per nucleon [10]. This is consistent with the most probable momentum for protons that varies between 1–15 GeV/c during the orbit due to the latitude-dependent geomagnetic cutoff [7].

The solar panels can be approximated as 1 mm of silicon with $A = 25$, hence their spallation π^- production can be approximated as 1 mm/10 cm = 1% that of the rest of *Mir*. Since the observed $Z = -1$ flux from *Mir* is 6 times that of the observed ambient cosmic ray electron flux, the contribution of the solar panels has to be 6% that of cosmic ray electron flux. Such a small contribution is difficult to detect and explains why the solar panels appear invisible on the projection plots.

5. Conclusion

The AMS-01 experiment detected a μ^- and π^- flux from cosmic ray nuclei interacting with the *Mir* space station. The precision tracker allowed the arrival directions of cosmic rays to be binned such that an image is generated on which individual *Mir* modules can be distinguished by their flux of short-lived μ^- and π^-.

During the AMS-02 experiment we expect parts of the ISS and support vehicles to be within the detector's field of view. This result shows that we can use the data directly, without resorting to expensive and less reliable simulation, to identify these parts. Using a simple graphical test based on this imaging technique, affected regions in the AMS-02 field of view may be removed from sensitive analysis.

[10] This is substantially thicker than the hull of *Mir*, but accounts for the equipment inside the hull.

Acknowledgements

The success of the first AMS mission is due to many individuals and organizations outside the collaboration. The support of NASA and the US Department of Energy has been vital in the inception, development and operation of the experiment. The interest and support of Mr. Daniel S. Goldin, former NASA Administrator, is gratefully acknowledged. The dedication of Dr. John O'Fallon, Dr. Peter Rosen and Dr. P.K. Williams of US DOE, our Mission Management team, Dr. Douglas P. Blanchard, Mr. Mark J. Sistilli and Mr. James R. Bates, NASA, Mr. Kenneth Bollweg and Mr. T. Martin, Lockheed-Martin, the support of the space agencies from Germany (DLR), Italy (ASI), France (CNES) and China (CALT) and the support of CSIST, Taiwan, made it possible to complete the experiment on time.

We are most grateful to the STS-91 astronauts, particularly Dr. Franklin Chang-Diaz who provided help to AMS during the flight.

References

[1] J. Alcaraz et al., Phys. Lett. B 461 (1999) 387.
[2] J. Alcaraz et al., Phys. Lett. B 472 (2000) 215.
[3] J. Alcaraz et al., Phys. Lett. B 494 (2000) 193.
[4] J. Alcaraz et al., Phys. Lett. B 484 (2000) 10.
[5] J. Alcaraz et al., Phys. Lett. B 490 (2000) 27.
[6] <http://spaceflight.nasa.gov/history/shuttle-mir/index.html>.
[7] M. Aguilar et al., Phys. Rep. 366 (2002) 331.
[8] J.C. Hart, D.H. Saxon, Nucl. Instr. and Meth. 220 (1984) 309.
[9] A. Moiseev, J. Ormes, Astropart. Phys. 6 (1997) 379.
[10] M. Gaździcki, D. Röhrich, Z. Phys. C 65 (1995) 215.